Free Radical Research, July 2010; 44(7): 751–762

informa
healthcare

Effect of 2, 5- substituents on the stability of cyclic nitrone superoxide spin adducts: A density functional theory approach

LI-BO DU[1], LAN-FEN WANG[1], YANG-PING LIU[1,2], HONG-YING JIA[1], YANG LIU[1], KE-JIAN LIU[3] & QIU TIAN[1]

[1]*State Key Laboratory for SCUSS, Institute of Chemistry, The Chinese Academy of Sciences, Beijing 100190, PR China,* [2]*Center for Biomedical EPR Spectroscopy and Imaging, The Davis Heart and Lung Research Institute, the Division of Cardiovascular Medicine, Department of Internal Medicine, The Ohio State University, Columbus, OH 43210, USA, and* [3]*College of Pharmacy University of Mexico, Albuquerque, NM 87131, USA*

(Received date: 11 February 2010; In revised form date: 8 March 2010)

Abstract

In the present study, five cyclic nitrone superoxide spin adducts, i.e. DMPO-OOH, M_3PO-OOH, EMPO-OOH, DEPMPO-OOH and DEPDMPO-OOH, were chosen as model compounds to investigate the effect of 2,5-subsitituents on their stability, through structural analysis and decay thermodynamics using density functional theory (DFT) calculations. Analysis of the optimized geometries reveals that none of the previously proposed stabilizing factors, including intramolecular H-bonds, intramolecular non-bonding interactions, bulky steric protection nor the C(2)–N(1) bond distance can be used to clearly explain the effect of 2,5-substituents on the stability of the spin adducts. Subsequent study found that spin densities on the nitroxyl nitrogen and oxygen are well correlated with the half-lives of the spin adducts and consequently are the proper parameters to characterize the effect of 2,5-substituents on their stability. Examination of the decomposition thermodynamics further supports the effect of the substituents on the persistence of cyclic nitrone superoxide spin adducts.

Keywords: Spin trapping, DFT calculations, superoxide anion, nitrone.

Abbreviations: *DMPO, 5,5-dimethyl-1-pyrroline* N*-oxide; DEPMPO, 5-diethoxy phosphoryl-5-methyl-1-pyrroline* N*-oxide; EMPO, 5-ethoxycarbonyl-5-methyl-1-pyrroline* N*-oxide; M_3PO, 2,5,5-trimethyl-1-pyrroline*-N*-oxide; DEPDMPO, 5-(diethoxy phosphoryl) -2,5-dimethyl-1-pyrroline*–N*-oxide*.

Introduction

Electron spin resonance (ESR) in combined with the spin trapping technique, as one of the useful methods to detect superoxide radical and other reactive oxygen species, has been extensively employed to probe and characterize the free radical processes in chemical and biological systems. To efficiently detect the free radicals in biological systems, the spin trap used should trap radicals rapidly, resulting in a long-lived radical spin adduct. The cyclic nitrone DMPO is one of the most commonly used spin traps [1,2]. However, its extensive application in biological milieu has been restricted due to the low superoxide trapping rate (1.2 $M^{-1}s^{-1}$ at pH 7.4) [3,4] and the low stability of the corresponding superoxide spin adduct ($t_{1/2} \approx 1.0$ min) [5,6]. Therefore, the molecular structure of DMPO has been systematically modified and various cyclic nitrone analogues obtained. For example, introducing the substituents $P(O)(OCH_2CH_3)_2$ or $COOCH_2CH_3$ affords alkoxyphosphoryl-nitrone DEPMPO [7,8] and alkoxycarbonyl-nitrone EMPO [9,10], respectively. Both DEPMPO and EMPO exhibit a significant improvement in the spin-trapping rate for superoxide radical and the stability of their corresponding superoxide spin adducts [11,12] and both have been widely used in radical detection in chemistry and biology research [13,14].

Correspondence: Yang Liu, State Key Laboratory for SCUSS, Institute of Chemistry, The Chinese Academy of Sciences, Beijing 100080, PR China. Tel: +86-010-62571074. Fax: +86-010-62559373. Email: yliu@iccas.ac.cn

ISSN 1071-5762 print/ISSN 1029-2470 online
DOI: 10.3109/10715761003758130

The persistence of the superoxide spin adduct is an even more important factor in the above-mentioned criterion (i.e. the superoxide spin-trapping rate and the stability of the superoxide adduct). Therefore, many efforts have been made toward elucidating the stabilizing role of the strong electron-withdrawing alkoxyphosphoryl and alkoxycarbonyl groups regarding the superoxide spin adducts. Tordo and Nohl [15,16] experimentally suggested that the strong electron-withdrawing effect and the large steric hindrance of the alkoxyphosphoryl group or alkoxycarbonyl group were responsible for the stability of the linear and cyclic nitrone spin adducts. Vellamena's theoretical data [17–19] further revealed that the intramolecular H-bond played an important role in the stability of the superoxide and hydroxyl spin adducts. In analysis of the phosphoryl effect on the stability of linear nitrone superoxide spin adducts, we found that besides the aforementioned stabilizing factors, the intra-molecular non-bonding interaction may be another contributing factor to the stabilization of the linear nitrone superoxide spin adducts [20]. Taken together, the large steric hindrance, intra-molecular H-bonding and non-bonding interactions induced by the strong electron-withdrawing groups are all possible structural factors that contribute to the stabilization of superoxide spin adducts.

In vivo, the radical spin-trapping capability of nitrones is not only dependent on the static stabilizing effect on the resulting adducts, but is also associated with the spin adducts' surrounding environments. Previous studies [21–23] found that radical ($\cdot CH_3$, $\cdot CO_2^-$, $\cdot OH$, etc.) adducts of M_3PO, obtained by replacing the β-H of DMPO with a methyl group, are far more stable and less susceptible to cellular-induced destruction than the corresponding DMPO adducts. However, the M_3PO superoxide spin adduct is too unstable to be directly detected by ESR at room temperature [21–23]. To design a better spin trap for superoxide radicals on the basis of M_3PO molecular skeleton, we previously synthesized its phosphoryl analogue, DEPDMPO, through incorporation of one phosphoryl group at the C-5 position [24]. ESR results indicated that the half-life of the superoxide spin adduct DEPDMPO-OOH is 2.6 min, which is much longer than that of M_3PO-OOH. Comparative analysis of the half-lives of DMPO-OOH/M_3PO-OOH and DEPMPO-OOH/DEPDMP-OOH further indicates that the introduction of a methyl group at the C-2 position is not beneficial to the stability of DMPO-type superoxide spin adducts.

Consequently, in order to have a better understanding of the effects of having a 2-methyl group and strong electron withdrawing groups at the 5 position, briefly referred to as 2,5-substituents, on the persistence of the superoxide spin adducts and to reveal the correlation of such substitutions with the intrinsic structural features of the spin adducts, we herein comparatively analyse and discuss the geometric and electronic structures, as well as several possible decomposition pathways of five superoxide spin adducts DMPO-OOH, M_3PO-OOH, EMPO-OOH, DEPMPO-OOH and DEPDMPO-OOH (Scheme1). Our goal in this paper was accomplished by virtue of the density functional theory (DFT) calculation method CPCM-B3LYP/6-311+G(d,p)//B3LYP/6-31G(d).

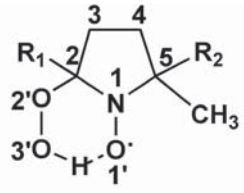

Spin adduct	R_1	R_2
DMPO-OOH	H	CH_3
M_3PO-OOH	CH_3	CH_3
EMPO-OOH	H	CO_2Et
DEPMPO-OOH	H	$P(O)(OEt)_2$
DEPDMPO-OOH	CH_3	$P(O)(OEt)_2$

Scheme 1. Molecular structures of superoxide spin adducts.

Experimental

Materials

According to the reported literature methods, DMPO [1,2], M_3PO [1], EMPO [10], DEPMPO [7] and DEPDMPO [24] were synthesized in our laboratory. Tetracyanoethylene (TCNE), Superoxide Dismutase (SOD), Catalase and Diethylenetriamine pentaacetic acid (DTPA) were purchased and used without further purification. PSII membranes obtained from market spinach were isolated by the method of Berthold et al. [25] with the modification of Yruela et al. [26].

Decay dynamics of superoxide spin adducts

The light-PSII system is utilized to investigate the kinetics of decay for the superoxide spin adducts [27–29]. Phosphate buffer solution (0.1 M, pH 7.0) containing PSII (0.45 mg Chl/ml), spin trap (50 mM), TCNE (1 mM) and DTPA (1 mM) is illuminated by He-Ne laser (25 mW, 633 nm) for 2 min. Once the light source was shut off, the decay of the superoxide spin adduct was followed by monitoring the decrease of the intensity of the first low field ESR line. Simulation of an approximate first-order decay process was carried out by Origin7.0 software. The peak intensity of the detected ESR signal is related to the actual concentration of the spin adduct by a scaling factor. The ESR spectra are recorded with the following parameters: frequency modulation, 100 kHz; modula-

tion amplitude, 2 Gauss; scan time, 42 s; time constant, 0.16 s; microwave power, 12.8 mW.

Computational methods

Considering the accuracy and convenience of density functional theory (DFT) [30,31], the B3LYP function on the basis set of 6-31G (d) is employed to carry out calculations. First, molecular geometries are optimized by semi-empirical quantum chemical method AM1. Then, B3LYP/6-31G (d) is used for the full geometry optimization in gas phase. All stable structures predicted without virtual vibrational frequencies are gained. Zero point vibrational energy (ZPVE) and the vibrational contribution to the enthalpy and entropy are scaled by a factor of 0.9806 [32]. Single point energies are obtained using B3LYP/6-311+G (d,p). To resolve the basis set dependence problem encountered in the Mulliken population analysis, five basis sets, i.e. 6-31+G(d,p), 6-311+G(d,p), 6-311++G(d,p), 6-311+G(2d,2p) and 6-311++G(2d,2p), are used to calculate Mulliken charges and spin densities. Therein, the solvent effects are also considered by employing the self-consistent reaction field (SCRF) method with conductor-like polarizable continuum model (CPCM) [33]. All quantum chemical calculations are performed with Gaussian 98 [34].

Results and discussion

Decay kinetics of superoxide spin adducts

The stability of the superoxide spin adduct is one of the most crucial factors for designing a desirable superoxide spin trap and, thus, the half-life ($t_{1/2}$) is commonly used to evaluate its performance. However, the previously reported $t_{1/2}$s regarding the five superoxide spin adducts studied in this work were not obtained in an identical experimental condition [5–7, 10,11,35]. In order to comparatively investigate the substituent effects on their stability, as listed in the first row of Table I, the $t_{1/2}$s are re-examined under uniform conditions. As expected, M_3PO-OOH was too unstable to be detected by ESR spectroscopy. In the case of DEPDMPO-OOH, only the *trans*-isomer was observed due to the steric hindrance of the alkoxyphosphoryl and methyl groups, which forces the superoxide radical to attack the C=N bond only from the opposite side of the alkoxyphosphoryl group. As shown in Figure 1A, the ESR spectrum of DEPDMPO-OOH (a_N = 1.34 mT, a_P = 5.05 mT) was obtained by the light-PSII system. However, no ESR signal was detectable upon the addition of SOD (Figure 1B), which confirms that the ESR signal shown in Figure 1A is due to the trapping of superoxide. On the other hand, trapping hydroxyl radical using Fenton system led to the detection of a persistent signal shown in Figure 1C (a_N = 1.46 mT, a_P = 4.68 mT). The signal could be inhibited by the presence of catalase (50 U/mL) in the Fenton system (Figure 1D). The introduction of a methyl group at the C-2 position not only eliminates the presence of the *cis*-isomer, but also removes the β-H splittings from the ESR spectra for both spin adducts. Both factors lead to a simplified ESR spectrum with higher resolution. Remarkable differences in $t_{1/2}$ values among DEPMPO-OOH (14.8 min), EMPO-OOH (8.6 min) and DMPO-OOH (56 s) indicates that the incorporation of an electron-withdrawing group at the C-5 position

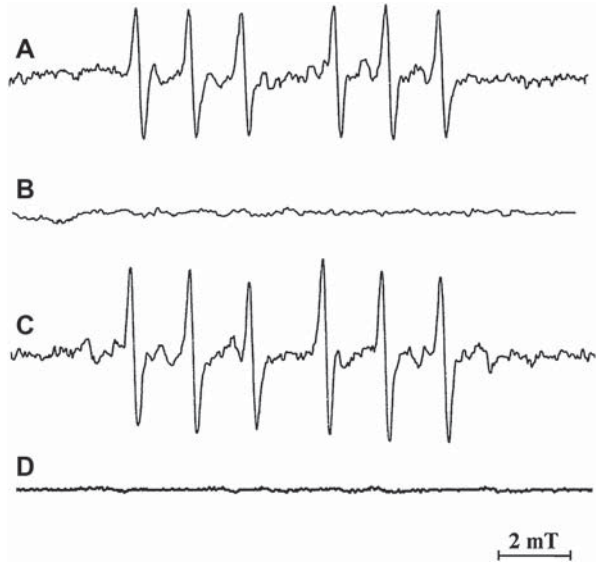

Figure 1. The ESR spectra of DEPDMPO's spin adducts. (A) Obtained in the mixture of phosphate buffer solution (0.1 M, pH 7.0) containing PSII (0.45 mg Chl/ml), DEPDMPO (50 mM), TCNE (1 mM) and DTPA (1 mM) under He-Ne laser illumination (25 mW, 633 nm, 2 min); (B) As in (A) but in the presence of SOD (1000 U/mL); (C) Obtained in the mixture of phosphate buffer solution (0.1 M, pH 7.4) containing H2O2 (1 mM), FeSO4 (0.3 mM) and DEPDMPO (50 mM); (D) As in (C) but in the presence of Catalase (50 U/mL)

Table I. Half-lives ($t_{1/2}$) and ESR hyperfine splitting constants (A_N) for the superoxide spin adducts in phosphate buffer (0.1 M, pH = 7.0).

Spin adduct	DMPO-OOH	M_3PO-OOH	EMPO-OOH	DEPMPO-OOH	DEPDMPO-OOH
$t_{1/2}$ (min)	56s; this work	—	8.0; this work	14.0; this work	2.1; this work
	1.0; ref. 1b	—	8.0; ref. 4a	14.0; ref. 3a	2.6; ref. 11
	54s; ref. 2c		4.8; ref. 4b	14.2; ref. 2c	
	50s; ref. 18		8.6; ref. 4c	14.8; ref. 3b	
				13.0; ref. 18	
A_N(G)	14.3	—	13.3	13.2	13.4

of cyclic nitrones increases the stability of the corresponding superoxide spin adduct. Considering that DEPMPO-OOH has a much longer half-life than EMPO-OOH, it seems that the stabilizing effect of the alkoxyphosphoryl group is stronger than that of the alkoxycarbonyl group. Comparative investigation revealed that the introduction of an electron-donating methyl group at the C-2 position of nitrones decreases the stability of the spin adducts. For example, both DEPDMPO-OOH (2.1 min) and M_3PO-OOH (undetectable) have smaller $t_{1/2}$s in comparison with DEPMPO-OOH and DMPO-OOH, respectively.

Structural stability of superoxide spin adducts

Analysis of the optimized geometry of superoxide spin adducts. Intra-molecular H-bonding, non-bonding interactions, as well as large steric hindrance induced by strong electron-withdrawing groups, as mentioned in the Introduction, are all possible structural factors which can stabilize linear nitrone superoxide spin adducts. Thus, in order to theoretically elucidate the effect of 2, 5-substituents on the stability of the superoxide spin adducts, in the following sections we attempt to analyse these three stabilizing factors based on their optimized geometries. Two optimized configurations, i.e. *cis*- and *trans*-isomers, are assigned for DEPMPO-OOH and EMPO-OOH, indicating the position of the alkoxyphosphoryl or alkoxycarbonyl groups relative to the OOH group.

The calculated intra-molecular H-bonds (IHB) between hydrogen of the OOH group and oxygen of the nitroxyl, alkoxyphosphoryl and alkoxycarbonyl groups are in the range of 1.814~2.100 Å (Table II). Herein, IHBs for DMPO-OOH, EMPO-OOH and DEPMPO-OOH are similar to previously reported values [18,36]. The IHB for *cis*-DEPMPO-OOH (1.814 Å) is shortest, indicating that the alkoxyphosphoryl group is the best among the studied groups to stabilize the superoxide spin adducts through IHB. Further analysis shows that EMPO-OOH, however, has weaker IHBs (1.987 Å for *trans*-isomer and 2.100 Å for *cis*-isomer) than DMPO-OOH (1.959 Å), paradoxically inconsistent with their stability. This implies that intra-molecular H-bonding is unable to explain the effect of the substituent at C-5 on the stability of the superoxide spin adducts. A similar result is also observed for the methyl at C-2. For instance, less stable M_3PO-OOH (1.933 Å) affords a stronger IHB than DMPO-OOH (1.959 Å) does. Therefore, although IHBs may play an important role in stabilizing the superoxide spin adducts, it cannot be used to fully interpret the substituent effect at 2, 5-positions.

Examination of intra-molecular non-bonding interactions indicates that many interactions are present in the molecular structure of the superoxide spin adducts and their distances vary from 2.293–2.973 Å (Table III), which falls within the range of previously proposed non-bonding interactions (2.591~2.963 Å) [37]. The alkoxyphosphorylated and alkoxycarbonylated spin adducts, such as DEPMPO-OOH and EMPO-OOH, afford stronger intra-molecular non-bonding interactions compared to DMPO-OOH, implying that the electron-withdrawing groups at the C-5 position increase the stability of the superoxide spin adducts through intra-molecular non-bonding interactions. However, the introduction of a methyl group at the C-2 position enhances the intra-molecular non-bonding interaction in DEPDMPO-OOH or M_3PO-OOH when compared to DEPMPO-OOH or DMPO-OOH, respectively. As a result, the intra-molecular non-bonding interaction is obviously in contradiction with the destabilizing role of the methyl group for the spin adducts.

Inspection into the optimized geometry of DEPMPO-OOH shows that the alkoxyphosphoryl group is held in close proximity to the hydroperoxyl and nitroxyl groups. The steric proximity can be evidently demonstrated by comparison of some spatial angles around C (5). For example, the angle of N (1)-C (5)-P (106.6° for *trans*-isomer and 106.7° for *cis*-iso-

Table II. Intramolecular H-bonds (including O-H—O-N, O-H—O=P and O-H—O=C) calculated by B3LYP/6-31G(d).

	H-bond distance (Å)	
Spin adduct	This work	Ref. 8b
DMPO-OOH	1.959	1.99
M_3PO-OOH	1.933	
EMPO-OOH	1.987-*trans*;[a] 2.100-*cis*[b]	1.99-*trans*;[a] 2.00-*cis*[b]
DEPMPO-OOH	2.076-*trans*;[a] 1.814-*cis*[c]	2.00-*trans*;[a] 1.91-*cis*[c]
DEPDMPO-OOH	1.963	

[a]O-H—O-N. [b]O-H—O=C. [c]O-H—O=P.

Table III. Selected nonbonding distances (Å) in the optimized geometries of superoixde spin adducts at the B3LYP/6-31G(d) level of theory.

Spin adduct	Distances (Å)
M_3PO-OOH	2.300, 2.524, 2.663, 2.696, 2.720, 2.795, 2.827, 2.988
DMPO-OOH	2.375, 2.404, 2.704, 2.727, 2.803
Trans-EMPO-OOH	2.409, 2.488, 2.508, 2.534, 2.600, 2.627, 2.642, 2.657, 2.733, 2.777, 2.973
Cis-EMPO-OOH	2.319, 2.541, 2.570, 2.613, 2.626, 2.632, 2.657, 2.658, 2.667, 2.713, 2.954
Trans-DEPMPO-OOH	2.411, 2.480, 2.539, 2.547, 2.579, 2.641, 2.645, 2.671, 2.689, 2.694, 2.697, 2.729, 2.737, 2.751, 2.769, 2.904, 2.939
Cis- DEPMPO-OOH	2.545, 2.581, 2.612, 2.612, 2.623, 2.643, 2.643, 2.696, 2.698, 2.708, 2.720, 2.724, 2.758, 2.784, 2.800, 2.874, 2.910, 2.960
DEPDMPO-OOH	2.427, 2.500, 2.532, 2.546, 2.594, 2.638, 2.654, 2.672, 2.694, 2.696, 2.701, 2.706, 2.724, 2.729, 2.763, 2.766, 2.768, 2.885, 2.899, 2.936

mer) is smaller than the usual bond angle of sp^3 hybrid orbital (109.5°). It can be thus determined that the large alkoxyphosphoryl group provides steric protection towards two vulnerable groups, -OOH and nitroxyl, by preventing or inhibiting the attack from other molecules (e.g. water) in the solution and, therefore, stabilizes the spin adduct. Similarly, this steric protection also occurs in the structures of the other four superoxide spin adducts. As shown in Table IV, the order for the corresponding spatial angle N(1)-C(5)-P (or C) is DEPDMPO-OOH (106.3°) < DEPMPO-OOH (106.6° for *trans*-isomer and 106.7° for *cis*-isomer) < EMPO-OOH (106.4° for *trans*-isomer and 107.3° for *cis*-isomer) < DMPO-OOH (108.9°) ~ M_3PO-OOH (108.9°). It is therefore concluded that an alkoxyphosphoryl group substituted at the C-5 position has stronger protection than either alkoxycarbonyl or methyl groups, because of the larger steric volume, explaining the better stability of DEPMPO-OOH, compared to that of EMPO-OOH and DMPO-OOH, and also the better stability of DEPDMPO-OOH when compared to that of M_3PO-OOH. However, in comparison to the C-5 substitution, the methyl group substituted at the C-2 position has almost no effect on varying the spatial angles (N(1)-C(5)-P of DEPDMPO-OOH and N(1)-C(5)-C of M_3PO-OOH), which probably means that the C-2 substitution does not affect the stability via the means of steric protection.

The above analyses demonstrate that intra-molecular H-bonds, intra-molecular non-bonding interactions, as well as steric protection may be important factors that contribute to stabilizing the superoxide spin adducts, but they cannot be used to fully elucidate the effects of 2,5-subsituents on the stability of the spin adducts. This encourages us to seek other better explanations.

The C (2)–N (1) bond has been reported to play a key role in the unimolecular decomposition process of nitrone radical adducts [17,38,39]. Thus, the C (2)–N (1) bond distance was chosen as another candidate to represent the 2, 5-substituents'effect. As listed in Table IV, the order of C(2)–N(1) bond distances is as follows: DEPDMPO-OOH (1.493Å) > M_3PO-OOH (1.492 Å) > DMPO-OOH (1.481 Å) > EMPO-OOH (1.480 Å-*cis*) > DEPMPO-OOH (1.474 Å-*cis*). Except for DEPDMPO-OOH, the order is the same as that for their stability profile. That is to say, introduction of an electron-withdrawing group at C-5 position shortens the C(2)–N(1) bond distance and then stabilizes superoxide spin adducts, but the addition of a methyl group at the C-2 position has an opposite effect.

Analysis of the optimized electronic structure of superoxide spin adducts. Chemical reactivity is not only closely related to the geometric structures of the reactants, but is also dominated by their electronic structures. It may therefore be expected that the changes in the electronic structures of superoxide spin adducts will vary the stabilities according to the effect from 2, 5-substituents.

It has been recently reported that a relatively negative charge on the nitroxyl nitrogen of the hydroxyl spin adducts, caused by a strong electron-withdrawing group at C-5 position, can stabilize the C–N bond and significantly increases the electronegativity of nitrogen through an inductive effect [17,40]. Our calculation (Table IV) reveals that either the Mulliken charge on the nitroxyl nitrogen for EMPO-OOH (0.0491-*cis*) or that for DEPMPO-OOH (0.0863-*cis*) is obviously lower than that for DMPO-OOH (0.1305), consistent with Villamena et al.'s [17,40] works. However, compared with DEPMPO-OOH, EMPO-OOH possesses an even lower charge on the nitroxyl nitrogen, which cannot be readily interpreted according to the stability difference. The methyl substituent at the C-2 position affords more positive charge on the nitroxyl nitrogen, as demonstrated by the following order: DEPDMPO-OOH (0.3027) > M_3PO-OOH (0.2476) > DMPO-OOH (0.1305) > DEPMPO-OOH (0.0863-*cis*). However, the order is

Table IV. Thermodynamic parameters for superoxide spin adducts calculated by CPCM-B3LYP/6-311+G(d,p)//B3LYP/6-31G(d).

	DMPO-OOH	M_3PO-OOH	EMPO-OOH	DEPMMPO-OOH	DEPDMPO-OOH
Milliken Spin Density on N (1)	0.4992	0.5090	0.4836-*trans* 0.4857-*cis*	0.4661-*trans* 0.4499-*cis*	0.4886
Milliken Spin Density on O (1')	0.4697	0.4658	0.4784-*trans* 0.4957-*cis*	0.4829-*trans* 0.5114-*cis*	0.4719
Milliken Chargeon N (1)	0.1305	0.2476	0.1638-*trans* 0.0491-*cis*	0.2268-*trans* 0.0863-*cis*	0.3027
Milliken Chargeon O (1')	−0.2638	−0.2305	−0.2044-*trans* −0.1477-*cis*	−0.1443-*trans* −0.0834-*cis*	−0.1068
Bond Angles (°) ofN (1)-C (5)- P (C)	108.9	108.9	106.4-*trans* 107.3-*cis*	106.6-*trans* 106.7-*cis*	106.3
Bond Lengths (Å) of N (1)-C (2)	1.481	1.492	1.481-*trans* 1.480-*cis*	1.482-*trans* 1.474-*cis*	1.493
Bond Lengths (Å) of O (2')-O (3')	1.455	1.455	1.454-*trans* 1.450-*cis*	1.454-*trans* 1.452-*cis*	1.454
Dihedral Angles (°) of O (1')-N (1)-C (2)-H	73.6		−62.4-*trans* 62.1-*cis*	−63.3-*trans* 43.6-*cis*	

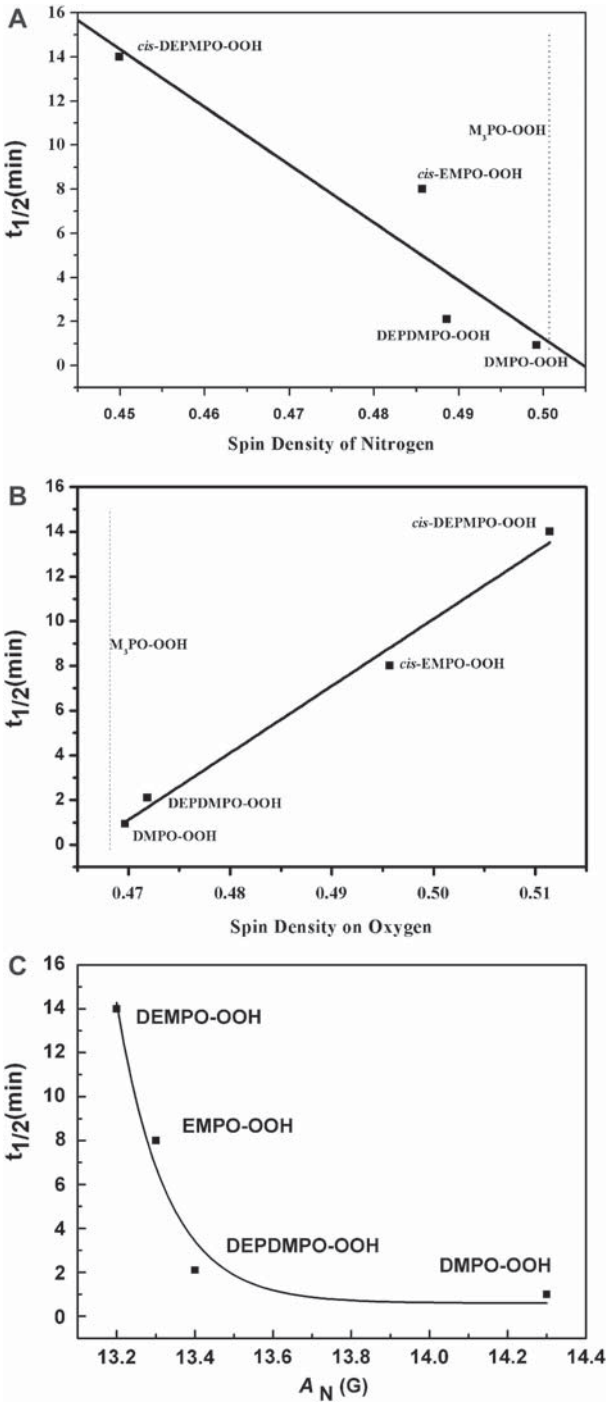

Figure 2. Plots of half-lives ($t_{1/2}$) of superoxide spin adducts vs spin densities on nitroxyl nitrogen (A) or nitroxyl oxygen (B) calculated at B3LYP/6-311+G(d,p) level and vs experimental hyperfine splitting constant of nitroxyl nitrogen (A_N) (C).

not identical to the stability sequence of all four adducts. As a result, the effect of the 2, 5-substituents on the stability of the superoxide spin adducts cannot be simply explained by the charge on the nitroxyl nitrogen. Similarly, we found that the charge on nitroxyl oxygen (Table IV) has no correlation with the stability of the superoxide spin adducts, either.

It is well known that the delocalization of the unpaired electron between the nitrogen and oxygen atoms of nitroxyl radical (N–O·) presents a resonance structure with $N^{\bullet+}$-$O^{-\bullet}$. Electron-withdrawing substituents at adjacent carbons increase spin density at the oxygen atom due to the increased role of the resonance structure with N–O· and as a result the oxygen has the lower charge [41]. There exists a lower spin density and higher charge at the nitrogen atom when a strong electron-withdrawing group binds at C-5 position. Considering the stabilizing effect of an electron-withdrawing substituent, such as an alkoxyphosphoryl or alkoxycarbonyl group, it is proposed that a relatively low spin density on the nitrogen atom probably stabilizes the superoxide spin adduct. The order of spin densities on the nitroxyl nitrogen (summarized in Table IV) can be obtained as follows: M_3PO-OOH (0.5090) > DMPO-OOH (0.4992) > DEPDMPO-OOH (0.4886) > EMPO-OOH (0.4836 for *trans*-isomer; 0.4857 for *cis*-isomer) > DEPMPO-OOH (0.4461 for *trans*-isomer; 0.4499 for *cis*-isomer). It is worth noting that the order is nearly identical to the stability sequence of all five spin adducts, which is evidence supporting the proposal about the stabilizing effect of spin density on the nitroxyl nitrogen. A quantitative linear correlation between spin densities on the nitrogen and the half-lives for the superoxide spin adducts is shown in Figure 2A (r = -0.8066). Therefore, it is concluded that the more stable the superoxide spin adduct, the lower the spin density on the nitroxyl nitrogen. Comparatively, the spin density on nitroxyl oxygen has a similarly positive correlation with the stability of the spin adducts (Figure 2B, r = 0.9851). It is known that Mulliken charges are basis set dependent and therefore four other basis sets was used to assess Mulliken charges and spin densities of nitroxyl nitrogen and oxygen (see Table V). As illustrated in Figure 2 and Table V, there are all those linear correlations between the half-lives for the superoxide spin adducts and the Mulliken spin densities either on nitrogen or oxygen nucleus derived with all five basis sets. Consequently, both spin densities on nitroxyl nitrogen and nitroxyl oxygen are good parameters that can be used to estimate the stability of the superoxide spin adducts.

It has been reported that the isotropic ESR hyperfine splitting constant (hfsc) is proportional to the unpaired spin electron density at the nucleus (Fermi contact terms) with an equation of $A_N = (8\pi/3h)g_N\beta_N g_e\beta_e\rho(0)$, where $\rho(0) = |\psi(0)|^2$ [42–44]. In actuallity, only the s-type orbital has non-zero electron density at the nucleus; all other-type orbitals (p-orbital, d-orbital and so on) have at least one node passing through the nucleus (zero density). Considering that the isotropic hyperfine splitting constant is proportional to the partial unpaired spin electron density (s-orbital), we may reasonably deduce that the half-lives ($t_{1/2}$) of the spin adducts would be negatively correlated with their hfs constants (A_N). This speculation is demonstrated by the plot of experimental A_N with $t_{1/2}$ of the adducts. As shown in Figure 2C, A_N

Table V. Mulliken charge and spin density for nitroxyl nitrogen and oxygen calculated by CPCM-B3LYP method at different basis set level.

	Milliken Charge N (1)	Milliken Chargeon O (1')	Milliken Spin Density on N (1)	Milliken Spin Density on O (1')
6-31+G(d,p)				
M_3PO-OOH	0.0483	−0.2374	0.5165	0.4434
DMPO-OOH	−0.0681	−0.2383	0.5121	0.4473
DEPDMPO-OOH	−0.2684	−0.0503	0.4903	0.4539
EMPO-OOH	−0.1395-*trans*	−0.1394-*trans*	0.4911-*trans*	0.4599-*trans*
	−0.0753-*cis*	−0.1691-*cis*	0.4818-*cis*	0.4822-*cis*
DEPMPO-OOH	−0.3204-*trans*	−0.0540-*trans*	0.4818-*trans*	0.4623-*trans*
	−0.1626-*cis*	−0.0911-*cis*	0.4561-*cis*	0.4903-*cis*
Linear correlations			$r = -0.8374$ ($p = 0.0557$)[a]	$r = 0.8977$ ($p = 0.0347$)[b]
6-311++G(d,p)				
M_3PO-OOH	0.2741	−0.2022	0.5070	0.4659
DMPO-OOH	0.1537	−0.2430	0.4946	0.4712
DEPDMPO-OOH	0.3550	−0.0576	0.4846	0.4747
EMPO-OOH	0.1284-*trans*	−0.1784-*trans*	0.4829-*trans*	0.4798-*trans*
	0.0575-*cis*	−0.1303-*cis*	0.4817-*cis*	0.4973-*cis*
DEPMPO-OOH	0.2588-*trans*	−0.1122-*trans*	0.4623-*trans*	0.4860-*trans*
	0.0405-*cis*	−0.0465-*cis*	0.4434-*cis*	0.5132-*cis*
Linear correlations			$r = -0.7973$ ($p = 0.0700$)[a]	$r = 0.9890$ ($p = 0.0037$)[b]
6-311+G(2d,2p)				
M_3PO-OOH	0.2533	−0.4224	0.5159	0.4549
DMPO-OOH	0.1501	−0.4392	0.5114	0.4590
DEPDMPO-OOH	0.1185	−0.2988	0.5013	0.4605
EMPO-OOH	0.1123-*trans*	−0.3766-*trans*	0.4974-*trans*	0.4688-*trans*
	0.1816-*cis*	−0.3736-*cis*	0.4927-*cis*	0.4921-*cis*
DEPMPO-OOH	0.0589-*trans*	−0.3193-*trans*	0.4893-*trans*	0.4699-*trans*
	−0.0856-*cis*	−0.3171-*cis*	0.4722-*cis*	0.4978-*cis*
Linear correlations			$r = -0.9347$ ($p = 0.0220$)[a]	$r = 0.8603$ ($p = 0.0477$)[b]
6-311++G(2d,2p)				
M_3PO-OOH	0.2853	−0.4023	0.5151	0.4540
DMPO-OOH	0.1819	−0.4228	0.5084	0.4599
DEPDMPO-OOH	0.1322	−0.2568	0.5008	0.4613
EMPO-OOH	0.0998-*trans* 0.2082-*cis*	−0.3588-*trans*	0.4972-*trans*	0.4692-*trans*
		−0.3660-*cis*	0.4909-*cis*	0.4924-*cis*
DEPMPO-OOH	0.0721-*trans*-0.1164-*cis*	−0.2899-*trans*	0.4877-*trans*	0.4714-*trans*
		−0.2992-*cis*	0.4681-*cis*	0.4981-*cis*
Linear correlations			$r = -0.9586$ ($p = 0.0139$)[a]	$r = 0.8616$ ($p = 0.0472$)[b]

[a]Correlation coefficient between spin densities on the nitrogen and the half-lives for the superoxide spin adducts; [b]Correlation coefficient between spin densities on the oxygen and the half-lives for the superoxide spin adducts.

exhibit an exponential correlation with $t_{1/2}$ of the spin adducts. This non-linearity probably arises from the fact that A_N is only proportional to the unpaired spin electron density of s-orbitals on the nitrogen atom.

Decay thermodynamics of superoxide spin adducts

Although an exhaustive empirical elucidation has been made of the decay mechanisms for cyclic nitrone radical adducts, especially superoxide spin adducts [2,45–48], its theoretical study has not received much attention. The interpretation of these decay mechanisms is valuable because it can be applied to the future development of efficient spin traps. Until recently only one study using DFT theory has shed light on the thermodynamics of decay for DMPO-OOH and DEPMPO-OOH [38]. To gain further insight into the effect of 2, 5-substituents on the stability of cyclic nitrone superoxide spin adducts and to design some new nitrones with better spin trapping properties, we therefore conducted DFT calculations for the possible decay thermodynamics of these five superoxide spin adducts.

C–N bond cleavage, as mentioned above, is generally involved in the unimolecular decomposition reaction of nitrone superoxide spin adducts [38,39]. Moreover, a few reports have revealed that C–H^{β} bond cleavage also occurs, both in the unimolecular decomposition of DMPO-OOH [49–51] or PBN-OOH [52] and in the bimolecular decay route for DEPMPO-OOH [53,54]. Meanwhile, the unimolecular reduction of nitroxide to the hydroxylamine should be taken into account when both an electron and a H^+ donor are present in the solution [20,34]. This type of reduction is a favourable route, especially in biological systems [55,56]. As a result, four possible decay routes, including three unimolecular pathways and one bimolecular pathway, have been analysed separately, as illustrated in Scheme 2. The calculated varieties of free energy (ΔG) including

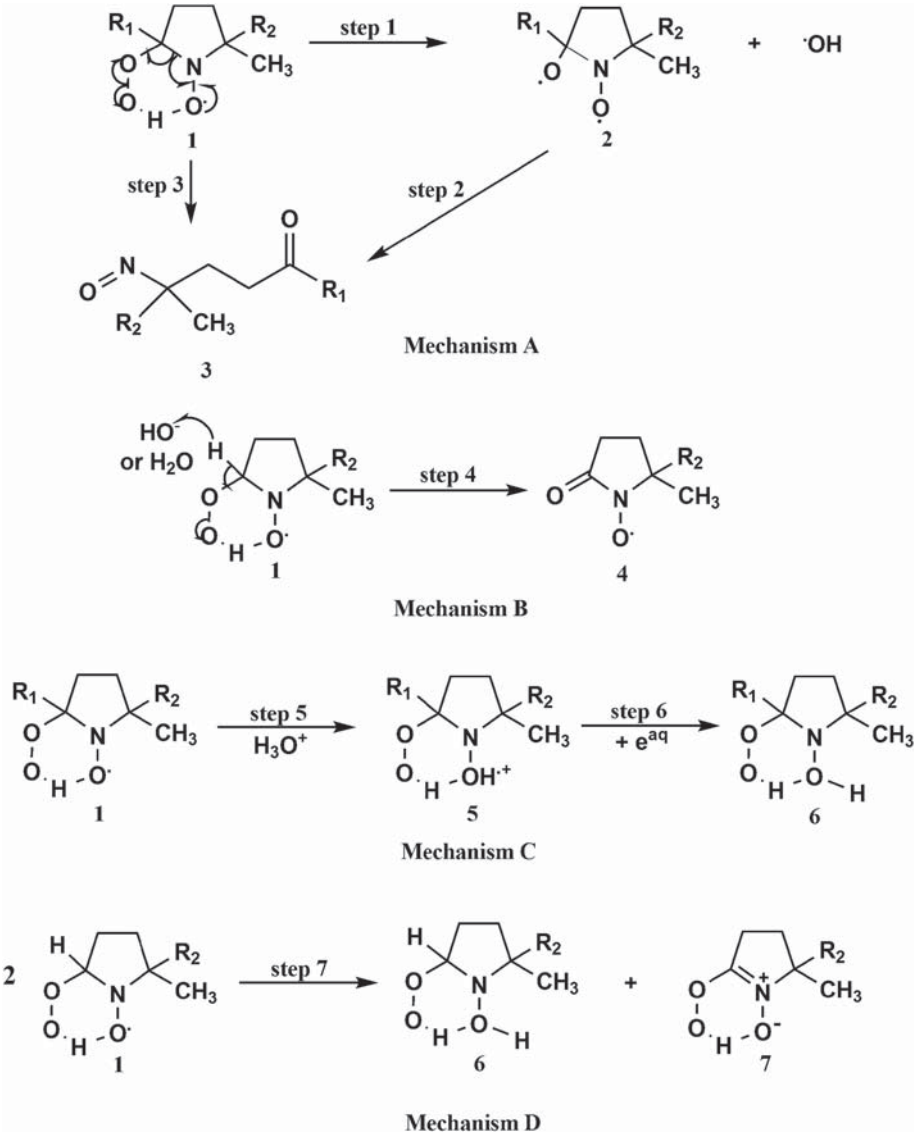

Scheme 2. Various possible decomposition pathways for superoxide spin adducts.

the effects of solvation, using the conductor-like polarizable continuum model (CPCM) are listed in Table VI. The schematic diagram of energy levels for ΔG in the rate-limiting steps of these decay routes are shown in Figure 3. The ΔG values described in the discussion are based on the most stable conformations (*cis*-isomers) for all five spin adducts. In addition, the solvent contribution to ΔG is listed in Table VII.

In the unimolecular decay process involving C–N bond cleavage (Mechanism A), superoxide spin adducts decompose through two steps [20,38,39]. The homolytic cleavage of the hydroperoxyl O–O bond (step 1) produces a diradical intermediate 2 (in singlet) and a hydroxyl radical and then the diradical 2 undergoes a C–N bond cleavage to yield a nitrosoaldehyde 3 (step 2) [38]. As usually observed during the decay of some superoxide spin adducts, the $HO^{\cdot}$ generated may then be trapped by the original nitrone to form a hydroxyl spin adduct [57,58]. Structural analysis of the superoxide spin adducts finds that the O–O bond lengths for all of the adducts are ~ 1.45Å, which is similar to the previously calculated values of cyclic nitrone superoxide spin adducts [35]. This implies that the likelihood of hydroxyl radical production from the O–O bond is the same for all of these superoxide spin adducts. Comparatively, as discussed above, the C(2)–N(1) bond distance varies dramatically and is simultaneously cleaved when the O–O bond is ruptured in step 1 on the basis of the structural diagram for diradical 2 (picture not shown). Accordingly, the C (2)–N (1) bond may play a key role in mechanism A, consistent with the previous proposal [17,38]. This implicitly suggests that step 1 is a rate-limiting step in mechanism A. This result is further strengthened by the fact that the diradical 2 and the final product, nitrosoaldehyde 3, share the same structure except for a difference in conformation. Thus, mechanism A was modified: the homolytic cleavages of the hydroperoxyl O-O bond and C-N bond produce a diradical intermediate 2 (in singlet)

Table VI. Reaction free energies (kcal/mol) of various decomposition pathways for superoxide spin adducts at the CPCM-B3LYP/6-311+G(d,p)//B3LYP/6-31G(d) level.

Reaction scheme	DMPO-OOH	M_3PO-OOH	EMPO-OOH	DEPMPO-OOH	DEPDMPO-OOH
Mechanism A					
Step 1	−2.77	−10.31	−3.81-*trans* 2.41-*cis*	−3.10-*trans* 0.85-*cis*	−12.15
Step 2	−1.29	−4.85	−1.97-*trans* −3.30-*cis*	−1.33-*trans* −3.39-*cis*	−2.89
Step 3	−4.05	−15.16	−5.78-*trans* −0.89-*cis*	−3.88-*trans* −2.54-*cis*	−15.04
Mechanism B					
Step 4	−86.25		−83.55-*trans* −83.49-*cis*	−84.65-*trans* −82.76-*cis*	
Mechanism C					
Step 5	11.93	10.08	12.03-*trans* 9.45-*cis*	9.41-*trans* 15.72-*cis*	9.99
Step 6	−128.37	−125.37	−129.72-*trans* −124.33-*cis*	−127.33-*trans* −133.29-*cis*	−128.31
Mechanism D					
Step 7	−39.12		−9.79-*trans* −9.68-*cis*	−11.16-*trans* −7.37-*cis*	

and a hydroxyl radical (step 1) and then the diradical 2 undergoes a configuration adjustment to yield a nitrosoaldehyde 3 (step 2). The order of $^{\cdot}G_1$ is as follows: EMPO-OOH (2.41 kcal/mol) > DEPMPO-OOH (0.85 kcal/mol) > DMPO-OOH (-2.77 kcal/mol) >> M_3PO-OOH (-10.31 kcal/mol) > DEDPMPO-OOH (-12.15 kcal/mol). Based on the order and the values of $^{\cdot}G_1$ (shown in Table VI and Figure 3), we can roughly speculate that an electron-withdrawing group at the C-5 position of a cyclic nitrone stabilizes its corresponding superoxide spin adduct by decreasing the reaction tendency described in mechanism A, whereas the methyl group at the C-2 position plays an opposite role.

The unimolecular decomposition process via the C–H$^{\beta}$ bond cleavage (mechanism B), possibly induced by HO^- or H_2O, yields a nitroxyl-ketone 4 through the elimination of a H_2O molecule (step 4) [38]. The

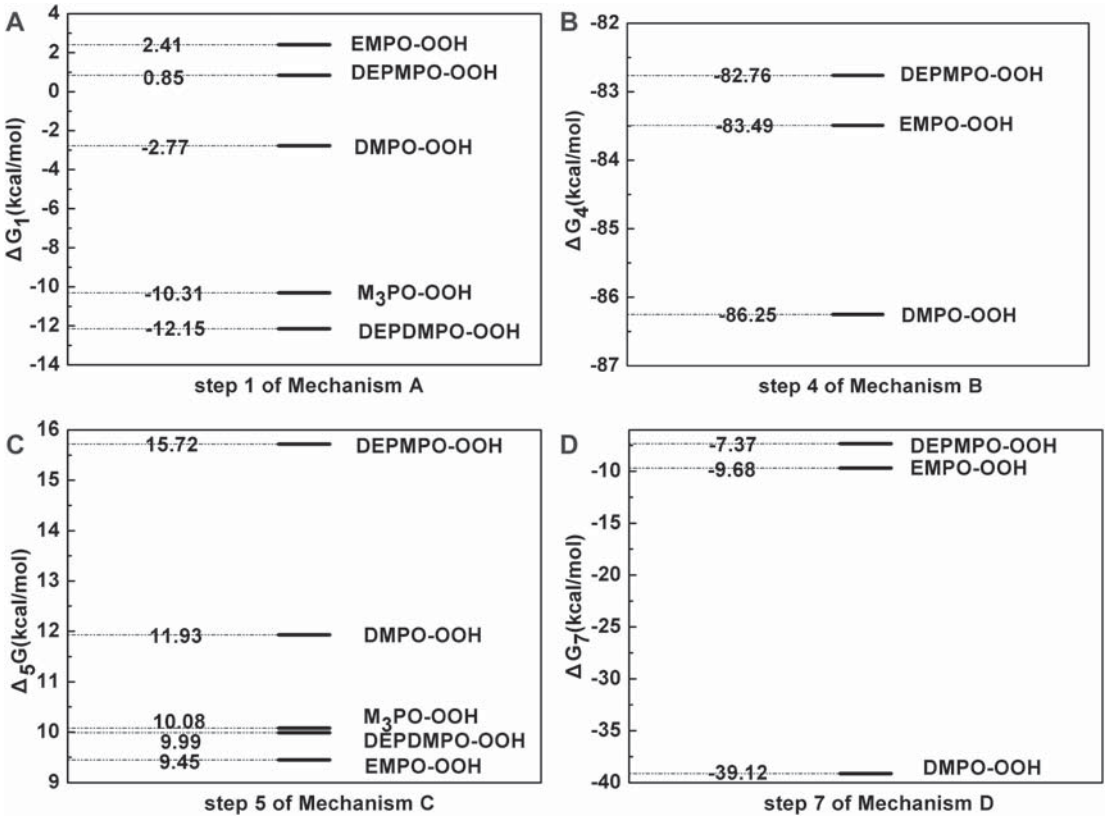

Figure 3. Energy level for reaction free energies (kcal/mol) in key steps of possible decomposition pathways (mechanisms A, B, C and D).

Table VII. Solvation contributions to reaction free energies (kcal/mol) of various decomposition pathways for superoxide spin adducts at the CPCM-B3LYP/6-311+G(d,p)//B3LYP/6-31G(d) level.

Reaction scheme	DMPO-OOH	M_3PO-OOH	EMPO-OOH	DEPMPO-OOH	DEPDMPO-OOH
Mechanism A					
Step 1	−1.38	−4.77	−0.65-*trans* −0.24-*cis*	−2.08-*trans* −1.56-*cis*	−7.19
Step 2	−0.86	0.16	−0.29-*trans* 0.45-*cis*	−1.15-*trans* −0.62-*cis*	−0.33
Step 3	−5.63	−1.22	−0.94-*trans* 0.21-*cis*	−3.23-*trans* −2.18-*cis*	−7.52
Mechanism B					
Step 4	−5.47		−5.31-*trans* −4.16-*cis*	−6.07-*trans* −5.02-*cis*	
Mechanism C					
Step 5	49.45	54.19	55.13-*trans* 59.14-*cis*	58.40-*trans* 61.27-*cis*	61.13
Step 6	49.42	43.84	43.81-*trans* 44.19-*cis*	39.76-*trans* 37.34-*cis*	35.63
Mechanism D					
Step 7	−39.12		−9.79	−11.16	

decomposition only occurs for DMPO-OOH, EMPO-OOH or DEPMPO-OOH, bearing a β-H at C-2 position. All calculated $\Delta G_{4,S}$ are less than -80.00 kcal/mol, significantly lower than $\Delta G_{1,S}$ and $\Delta G_{3,S}$ in mechanism A, which means that mechanism B is thermodynamically more feasible than the decomposition process via C-N cleavage. In mechanism B, the ΔG_4 is DMPO-OOH < EMPO-OOH < DEPMPO-OOH, which is identical with the observed decomposition tendency of the superoxide spin adducts. In other words, an electron-withdrawing group at the C-5 position can lessen the tendency to decay via C-H^β cleavage and therefore stabilize the superoxide spin adducts. It is shown that ease of the C-H^β bond cleavage for the HO· adduct was dependent on the conformation of the β-H relative to the singly occupied orbital on the nitroxyl nitrogen.[17] Only a low level of activation energy for the C-H^β cleavage is required when the singly occupied orbital on the nitroxyl nitrogen is in the same plane as the H^β atom to be abstracted. That is, the dihedral angle of < O(1')-N(1)-C(2)-H is close to 90°. Structural analysis shows that the more stable EMPO-OOH and DEPMPO-OOH have a smaller dihedral < O(1')-N(1)-C(2)-H (62.1° for *cis*-EMPO-OOH; 43.6° for *cis*-DEPMPO-OOH) than that of DMPO (73.6°). Correspondingly, an electron-withdrawing group at C-5 position decreases the likelihood of the decay via C-H^β bond cleavage.

In the unimolelcular reduction process (mechanism C), formation of a H-bond between an O atom from the nitroxyl group and a H^+ from H_3O^+ (step 5) is a pre-requisite and then the produced intermediate 5 accepts one electron and gives rise to hydroxylamine 6 (step 6). Although step 5 is endoergic (9.45 ~ 15.72 kcal/mol), the subsequent step 6 has a high exothermicity with ΔG_6 values of -124.33~-133.29 kcal/mol. A similar reduction mechanism has been proposed to possibly occur in the decay of the linear nitrone superoxide spin adducts and the protonation process is a rate-limiting step [20]. In step 5 (a protonation process), however, the order of ΔG_5 is EMPO-OOH < DEPDMPO-OOH~M_3PO-OOH < DMPO-OOH < DEPMPO-OOH (as shown in Table VI and Figure 3), largely inconsistent with their stability sequence. This result indicates that mechanism C probably is not the proper decay pathway that is responsible for elucidating the 2, 5-substituents' effect on the stability of cyclic nitrone superoxide spin adducts.

In the bimolecular decay pathway (mechanism D), the products were diamagnetic hydroxylamine 6 and compound 7. This is similar to the step 4 reaction in mechanism B, where the β-H abstraction reaction (step 7) takes place only in the decomposition processes of DMPO-OOH, EMPO-OOH and DEPMPO-OOH and, more interestingly, the ease of the β-H abstraction by another superoxide spin adduct molecule was postulated to be similarly dependent on the dihedral < O (1')-N (1)-C (2)-H [17]. Therefore, we can reasonably estimate the bimolecular decay tendency according to the dihedral angle (DMPO-OOH > EMPO-OOH > DEPMPO-OOH, see discussion for mechanism B). A comparison of ΔG_7 values calculated for mechanism D shows that the order of ΔG_7 is as follows: DEPMPO-OOH (-7.37 kcal/mol) > EMPO-OOH (-9.68 kcal/mol) > DMPO-OOH (-39.12 kcal/mol), which indicates that, in the bimolecular decomposition process, the introduction of a strong electron-withdrawing group at the C-5 position thermodynamically stabilizes the superoxide spin adduct.

Conclusions

Five cyclic nitrone superoxide spin adducts were utilized to investigate the effects of 2, 5-subsitituents on the stability of the superoxide spin adducts by employing DFT calculations. Analysis of their

geometric structures indicates that the previously suggested three factors, including intra-molecular H-bonds, intra-molecular non-bonding interactions and steric protection, may be important stabilizing factors for the superoxide spin adducts, but they are not available for fully predicting the effect of 2, 5-substituents on the stability. Further investigations on the stabilizing factors for the superoxide spin adducts indicate that neither the C(2)-N(1) bond distance nor the charges on the nitroxyl nitrogen and the nitroxyl oxygen are key parameters that can be used to explain the effects of 2,5-substituents.

Nevertheless, an inspection of the spin densities on nitroxyl nitrogen and nitroxyl oxygen reveals that both of their spin densities are linearly correlated with the stability of the superoxide spin adducts and thus probably used as proper parameters to interpret and predict the effects of 2, 5-substituents. Additional experimental analysis on the correlation between the hyperfine splitting constant of nitroxyl nitrogen (A_N) and the half-lives ($t_{1/2}$) of the spin adduct strongly support the hypothesis regarding the spin densities. On the other hand, thermodynamic calculations of the decay pathways, including three possible unimolecular decomposition processes and one possible bimolecular decomposition process, demonstrate that all the decay pathways, except for the unimolecular reduction of nitroxide to hydroxylamine, may be used in explaining the effects of 2,5-substituents on spin adduct stability.

Declaration of interest: The work was supported by the National High Technology Research and Development Program of China (863 program) (2007AA10Z352) and the National Natural Science Foundation of China (No. 90813021 & 20875093). The authors declare no conflict of interest. The authors alone are responsible for the content and writing of the paper.

References

[1] Bonnett R, Clark VM, Giddy A, Todd, A. Experiments towards the synthesis of corings. 1. the preparation and reactions of some delta-1-pyrrolines—a novel prolixne synthesis. J Chem Soc 1959;2087–2093.

[2] Haire DL, Hilborn JW, Janzen EG. A more efficient synthesis of DMPO-type (nitrone) spin traps. J Org Chem 1986;51: 4298–4300.

[3] Finkelstein E, Rosen GM, Rauckman EJ. Production of hydroxyl radical by decomposition of superoxide spin-trapped adducts. Mol Pharmacol 1982;21:262–265.

[4] Yamazaki I, Piette LH, Grover TA. Kinetics-studies on spin trapping of superoxide and hydroxyl radicals generated in NADPH-cytochrome-P-450 reductase-paraquat systems—effect of iron chelates. J Biol Chem 1990;265:652–659.

[5] Buettner GR, Oberley LW. Spin traps inhibit formation of hydrogen-peroxide via the dismutation of superoxide- implications for spin trapping the hydroxyl free-radical. Biochim Biophys Acta 1991;1075:213–222.

[6] Villamena FA, Zweier JL. Superoxide radical trapping and spin adduct decay of 5-tert-butoxycarbonyl-5-methyl-1-pyrroline N-oxide (BocMPO): kinetics and theoretical analysis. J Chem Soc Perkin Trans 2 2002;2:1340–1344.

[7] Frejaville C, Karoui H, Tuccio B, Lemoigne F, Culcasi M, Pietri S, Lauricella R, Tordo P. 5-Diethoxyphosphoryl-5-methyl-1-pyrroline N-oxide (DEPMPO)—a new phosphorylated nitrone for the efficient *in vitro* and *in vivo* spin trapping os oxygen-centered radicals. J Chem Soc Chem Commun 1994;15:1793–1794.

[8] Frejaville C, Karoui H, Tuccio B, Lemoigne F, Culcasi M, Pietri S, Lauricella R, Tordo P. 5-(Diethoxyphosphoryl)-5-methyl-pyroline N-oxide—a new efficient phosphorylated nitrone for the *in vitro* and *in vivo* spin-trapping of oxygen-centered radicals. J Med Chem 1995;38:258–265.

[9] Zhang H, Joseph J, Vasquez-Vivar J, Karoui H, Nsanzumuhire C, Martasek P, Tordo P, Kalyanaraman B. Detection of superoxide anion using an isotopically labeled nitrone spin trap: potential biological applications. FEBS Lett 2000;473:58–62.

[10] Olive G, Mercier A, Moigne FL, Rockenbauer A, Tordo P. 2-Ethoxycarbonyl-2-methyl-3,4-dihydro-2H-pyrrole-1-oxide: evaluation of the spin trapping properties. Free Radic Biol Med 2000;28:403–408.

[11] Tsai P, Ichikawa K., Mailer C, Pou S, Halpern HJ, Robinson BH, Nielsen R, Rosen G. Esters of 5-carboxyl-5-methyl-1-pyrroline N-oxide: a family of spin traps for superoxide. J Org Chem 2003;68:7811–7817.

[12] Lauricella R, Allouch A, Roubaud V, Bouteiller JC, Tuccio B. A new kinetic approach to the evaluation of rate constants for the spin trapping of superoxide/hydroperoxyl radical by nitrones in aqueous media. Org Biomol Chem 2004;2:1304–1309.

[13] Liu K, Sun J, Song YG, Liu B, Xu YK, Zhang SX, Tian Q, Liu Y. Superoxide, hydrogen peroxide and hydroxyl radical in D1/D2/cytochrome b-559 photosystem II reaction center complex. Photosyn Res 2004;81:41–47.

[14] Vasquez-Vivar J, Kalyanaraman B, Martasek P, Hogg N, Masters BSS, Karoui H, Tordo P, Pritchard KA. Superoxide generation by endothelial nitric oxide synthase: the influence of cofactors. Proc Natl Acad Sci USA 1998; 95:9220–9225.

[15] Tordo P. Spin-trapping: recent developments and applications. Electron Paramagn Reson 1998;16:116–144.

[16] Stolze K, Udilova N, Rosenau T, Hofinger A, Nohl H. Spin trapping of superoxide, alkyl- and lipid-derived radicals with derivatives of the spin trap EPPN. Biochem Pharmacol 2003; 66:1717–1726.

[17] Villamena FA, Hadad CM, Zweier JL. Theoretical study of the spin trapping of hydroxyl radical by cyclic nitrones: A density functional theory approach. J Am Chem Soc 2004;126:1816–1829.

[18] Villamena FA, Hadad CM, Zweier JL. Comparative DFT study of the spin trapping of methyl, mercapto, hydroperoxy, superoxide, and nitric oxide radicals by various substituted cyclic nitrones. J Phys Chem A 2005;109:1662–1674.

[19] Han YB, Tuccio B, Lauricella R, Rockenbauer R, Zweier JL, Villamena FA. Improved spin trapping properties by beta-cyclodextrin-cyclic nitrone conjugate. J Org Chem 2008; 73:2533–2541.

[20] Liu YP, Wang LF, Nie Z, Ji YQ, Liu Y, Liu KJ, Tian Q. Effect of the phosphoryl substituent in the linear nitrone on the spin trapping of superoxide radical and the stability of the superoxide adduct: Combined experimental and theoretical studies. J Org Chem 2006;71:7753–7762.

[21] Finkelstein E, Rosen GM, Rauckman EJ. Spin trapping kinetics of the reaction of superoxide and hydroxyl radicals with nitrones. J Am Chem Soc 1980;102:4994–4999.

[22] Janzen EG, Zhang YK. EPR spin trapping alkoxyl radicals with 2-substituted 5,5-dimethylpyrroline-N-oxides(2-XM2POS). J Magn Reson B 1993;101:91–93.

[23] Barasch D, Krishna MC, Russo A, Katzhendler J, Samuni A. Novel DMPO-derived C-13-labeled spin traps yield identifiable stable nitroxides. J Am Chem Soc 1994;116: 7319–7324.

[24] Xu YK, Sun J, Liu K, Chen ZW, Zhang XK, Liu Y. Structural analysis on superoxide spin adducts trapped by DEPMPO analogues. Chem J Chin Univ 2001;22:1732–1734.
[25] Berthold DA, Babcock GT, Yocum CF. A highly resolved, oxygen-evolving photosystem-II preparation from spinach thylakoid membranesp-electron-paramagnetic-res and electron-transport properties. FEBS Lett 1981;134:231–234.
[26] Yruela I, Montoya G, Alonso PA, Picorel R. Identification of the pheophytin-QA-FE domain of the reducing side of the photosystem-II as the Cu(II)-inhibitory binding-dite. J Biol Chem 1991;266:22847–22850.
[27] Buettner GR. Spin trapping: ESR parameters of spin adduct. Free Radic Res 1999;10:11–15.
[28] Liu K, Sun J, Liu Y, Zhang QY, Kuang TY. ESR studies on the superoxide radicals generated in photosystem II of higher plant. Prog Biochem Biophys 2001;28:372–374.
[29] Song YG, Liu B, Wang LF, Li MH, Liu Y. Damage to the oxygen-evolving complex by superoxide anion, hydrogen peroxide, and hydroxyl radical in photoinhibition of photosystem II. Photosynth. Res 2006;90:67–78.
[30] Labanowski JW, Andzelm J. Density functional methods in chemistry. New York: Springer; 1991.
[31] Parr RG, Yang W. Density functional theory in atoms and molecules. New York: Oxford University Press; 1989.
[32] Scott AP, Radom L. Harmonic vibrational frequencies: an evaluation of Hartree-Fock, Moller-Plesset, quadratic configuration interaction, density functional theory, and semiempirical scale factors. J Phys Chem 1996;100:16502–16513.
[33] Barone V, Cossi M. Quantum calculation of molecular energies and energy gradients in solution by a conductor solvent model. J Phys Chem A 1998;102:1995–2001.
[34] Frisch MJ, Trucks GW, Schlegel HB, Scuseria GE, Robb MA, Cheeseman JR, Zakrzewski VG, Montgomery JA, Jr Stratmann RE, Burant JC, Dapprich S, Millam J M, Daniels AD, Kudin KN, Strain MC, Farkas O, Tomasi J, Barone V, Cossi M, Cammi R, Mennucci B, Pomelli C, Adamo C, Clifford S, Ochterski J, Petersson GA, Ayala PY, Cui Q, Morokuma K, Salvador P, Dannenberg JJ, Malick DK, Rabuck AD, Raghavachari K, Foresman JB, Cioslowski J, Ortiz JV, Baboul AG, Stefanov BB, Liu G, Liashenko A, Piskorz P, Komaromi I, Gomperts R, Martin RL, Fox DJ, Keith T, Al-Laham MA, Peng CY, Nanayakkara A, Challacombe M, Gill PMW, Johnson B, Chen W, Wong MW, Andres JL, Gonzalez C, Head-Gordon M, Replogle E S, and Pople JA. Gaussian 98, revision A.11. Pittsburgh, PA: Gaussian, Inc; 2001.
[35] Roubaud V, Mercier A, Olive G, Moigne FL, Tordo P. 5-(Diethoxyphosphorylmethyl)-5-methyl-4,5-dihydro-3H-pyrrole N-oxide: synthesis and evaluation of spin trapping properties. J Chem Soc Perkin Trans 2 1997;9:1827–1830.
[36] Villamena FA, Merle JK, Hadad CM, Zweier JL. Superoxide radical anion adduct of 5,5-dimethyl-1-pyrroline N-oxide (DMPO). 1. The thermodynamics of formation and its acidity. J Phys Chem A 2005;109:6083–6088.
[37] Tsuzuki S, Uchimaru T, Tanabe K, Hirano T. Conformational-analysis of 1,2-dimethoxyethane by abinoton molecular-orbital and molecular mechanics calculations-stabilization of the TGG' rotamer by the 1,5-CH3/O nonbonding attractive interaction. J Phys Chem 1993;97:1346–1350.
[38] Villamena FA, Merle JK, Hadad CM, Zweier JL. Superoxide radical anion adduct of 5,5-dimethyl-1-pyrroline N-oxide (DMPO). 2. The thermodynamics of decay and EPR spectral properties. J Phys Chem A 2005;109:6089–6098.
[39] Finkelstein E, Rosen GM, Rauckman EJ. Production of hydroxyl radical by decomposition of superoxide spin-trapping adducts. Mol Pharm 1982;21:262–265.
[40] Villamena FA, Hadad CM, Zweier J. Kinetic study and theoretical analysis of hydroxyl radical trapping and spin adduct decay of alkoxycarbonyl and dialkoxyphosphoryl nitrones in aqueous media. J Phys Chem A 2003;107:4407–4414.
[41] Kocherginsky N, Swartz HM. Nitroxide spin labels. Reaction in biology and chemistry. New York, London, Tokyo: CRC Press: Boca Raton; 1995.
[42] Wertz JE, Bolton JR. Electron spin resonance elementary theory and practical applications. New York, London: Chapman and Hall; 1986.
[43] Villamena FA, Liu YP, Zweier JL. Superoxide radical anion adduct of 5, 5-dimethyl-1-pyrroline N-Oxide. 4. Conformational effects on the EPR hyperfine splitting constants. J Phys Chem A 2008;112:12607–12615.
[44] Cirujeda J, Vidal-Gancedo J, Jürgens O, Mota F, Movoa JJ, Rovira C, Veciana J. Spin density distribution of a-nitronyl aminoxyl radicals from experimental and *ab initio* calculated ESR isotropic hyperfine coupling constants. J Am Chem Soc 2000;122:11393–11405.
[45] Tordo P, Chalier F. 5-Diisopropoxyphosphoryl-5-methyl-1-pyrroline N-oxide, DIPPMPO, a crystalline analog of the nitrone DEPMPO: synthesis and spin trapping properties. J Chem Soc Perkin Trans 2 2002;2110–2113.
[46] Villamena FA, Rockenbauer A, Gallucci J, Velayutham M, Hadad CM, Zweier JL. Spin trapping by 5-carbamoyl-5-methyl-1-pyrroline N-oxide (AMPO): theoretical and experimental studies. J Org Chem 2004;69:7994–8004.
[47] Hardy M, Rockenbauer A, Vasquez-Vivar J, Felix C, Lopez M, Srinivasan S, Avadhani N, Tordo P, Kalyanaraman B. Detection, characterization, and decay kinetics of ROS and thiyl adducts of Mito-DEPMPO spin trap. Chem Res Toxicol 2007;20:1053–1060.
[48] Han Y, Tuccio B, Lauricella R, Rockenbauer A, Zweier JL, Villamena FA. Synthesis and spin-trapping properties of a new spirolactonyl nitrone. J Org Chem 2008;73:2533–2541.
[49] Finkelstein E, Rosen GM, Rauckman EJ. Spin trapping of superoxide. Mol Pharm 1979;16:676–685.
[50] Briere R, Rassat A. Nitroxides .68. synthesis and konetic dtudy of decomposition of T-butyl isopropyl nitroxide -isotope effect. Tetrahedron 1976;32:2891–2898.
[51] Villamena FA, Dickman MH, Crist DR. Stabilization of a nitroxide with a beta-hydrogen by metals: Structure and magnetic properties of adducts of N-oxy-N-tert-butyl-(2-pyridyl)phenylmethanamine with Mn(II), Ni(II), and Co(II) hexafluoroacetylacetonates. Inorg Chem 1998;37:1454–1457.
[52] Karoui H, Tordo P. ESR-spin trapping in the presence of cyclodextrins. Detection of PBN-superoxide spin adduct. Tetrahedron Lett 2004;45:1043–1406.
[53] Khramtsov V, Berliner LJ, Clanton TL. NMR spin trapping: detection of free radical reactions using a phosphorus-containing nitrone spin trap. Magn Reson Med 1999;42:228–234.
[54] Tuccio B, Lauricella R, Fréjaville C, Bouteiller JC, Tordo P. Decay of the hydroperoxyl spin adduct of 5-diethoxyphosphoryl-5-methyl-1-pyrroline N-oxode - an EPR kinetic-study. J Chem Soc Perkin Trans 2 1995;295–298.
[55] Gaffney BJ. Spin labeling theory and application. New York: Academic Press; 1976. p 183.
[56] Smith ICP. Biological applications of electron spin resonance. New York: Wiley-Interscience; 1972. p 483.
[57] Tuccio B, Bouteiller JC, Cerri V, Tordo P. Spin-trapping of free radicals by PBN-type beta-phosphorylated nitrones in the presence of SDS micelles. J Chem Soc Perkin Trans 2 1997;2507–2512.
[58] Karoui H, Clément JL, Rockenbauer A, Siri D, Tordo P. Synthesis and structure of 5,5-diethoxycarbonyl-l-pyrroline N-oxide (DECPO). Application to superoxide radical trapping. Tetrahedron Lett 2004;45:149–152.

This paper was first published online on Early Online on 30 May 2010.

Supplementary material available online